

1 Regional sea level change in response to ice mass loss 2 in Greenland, the West Antarctic and Alaska

S.-E. Brunnabend,^{1,2} J. Schröter,¹, R. Rietbroek,², and J. Kusche²

Corresponding author: S.-E. Brunnabend, Alfred-Wegener-Institut Helmholtz-Zentrum für Polar- und Meeresforschung, Bussestr. 24, 27570 Bremerhaven, Germany, now at University of Bonn, Institute for Geodesy and Geoinformation, Nussallee 17, 53115 Bonn, Germany (brunnabend@geod.uni-bonn.de)

¹Alfred-Wegener-Institut
Helmholtz-Zentrum für Polar- und
Meeresforschung, Bussestr. 24, 27570
Bremerhaven, Germany.

²University of Bonn, Institute for
Geodesy and Geoinformation, Nussallee 17,
53115 Bonn, Germany.

Abstract.

Besides the warming of the ocean, sea level is mainly rising due to land ice mass loss of the major ice sheets in Greenland, the West Antarctic and the Alaskan Glaciers. However, it is not clear yet how these land ice mass losses influence regional sea level. Here, we use the global Finite Element Sea-ice Ocean Model (FESOM) to simulate sea surface height (SSH) changes caused by these ice mass losses and combine it with the passive ocean response to varying surface loading using the sea level equation. We prescribe rates of fresh water inflow, not only around Greenland, but also around the West Antarctic Ice Sheet and the mountain glaciers in Alaska with approximately present day amplitudes of 200 Gt/yr, 100 Gt/yr and 50 Gt/yr, respectively. Perturbations in sea level and in freshwater distribution with respect to a reference simulation are computed for each source separately and in their combination. The ocean mass change shows an almost globally uniform behavior. In the North Atlantic and Arctic Ocean mass is redistributed toward coastal regions. Steric sea level change varies locally in the order of several centimeters on advective timescales of decades. Steric effects to local sea level differ significantly in different coastal locations, e.g. at North American coastal regions the steric effects may have the same order of magnitude as the mass driven effect, whereas at the European coast, steric effects remain small during the simulation period.

1. Introduction

24 Beside global mean sea level change, or more specifically, the increase in the volume and
25 mass of seawater, regional deviations from global mean sea level are of particular interest
26 for an observer at the coast [*Cazenave et al.*, 2008; *Church and White*, 2011]. Furthermore,
27 tide gauges are sensitive to relative sea level. It consists of changes in sea surface height
28 (SSH) and vertical land motion of the land. The latter is may be influenced by a mixture
29 of ongoing global isostatic adjustment (GIA), plate tectonics, subsidence of land due to the
30 withdrawal of ground water or oil and gas, or the compaction of sediments [*Bindoff et al.*,
31 2007]. Additionally, mass loss of land ice causes mass distribution changes on the Earth's
32 surface with an associated elastic response in uplift and geoid height. In the past five
33 decades, a major contribution to sea level rise has originated from the expansion of water
34 caused by warming of the ocean [*Levitus et al.*, 2005; *Gouretski and Koltermann*, 2007;
35 *Gregory et al.*, 2013]. In addition, in recent decades, the major ice sheets in Greenland
36 and West Antarctica have experienced increasing ice mass losses of hundreds of gigatons
37 per year (e.g. *Rignot et al.* [2008]; *Wu et al.* [2010]; *Jacob et al.* [2012]; *Gregory et al.*
38 [2013] and others). Furthermore, glaciers and ice-caps are melting [*Bindoff et al.*, 2007;
39 *Gregory et al.*, 2013]. In conclusion, ocean warming and land ice mass loss are both of
40 major importance when investigating sea level change in the global ocean.

41 To estimate the amount of mass loss of the ice sheets and glaciers, several studies have
42 been performed using different techniques ranging from ice sheet modeling to satellite
43 gravimetry and altimetry (*Wouters et al.* [2008]; *Gunter et al.* [2009]; *Jacob et al.* [2012];
44 *Velicogna et al.* [2014]; *Williams et al.* [2014]; *Schoen et al.* [2015] and others). During the

45 last decade, many studies indicate a mass loss between 100 Gt/yr and 150 Gt/yr of West
46 Antarctic Ice Sheet [Vaughan *et al.*, 2013; Rignot *et al.*, 2008; Chen *et al.*, 2009; Wu *et al.*,
47 2010; Jacob *et al.*, 2012; Velicogna *et al.*, 2014; Schoen *et al.*, 2015; van der Wal *et al.*,
48 2015], which is strongly dependent on the used GIA correction [Whitehouse *et al.*, 2012].
49 Regarding the Greenland Ice Sheet, an ice mass loss in the range of up to 278 Gt/yr has
50 been estimated for the last decade [Vaughan *et al.*, 2013; Luthcke *et al.*, 2006; Wouters
51 *et al.*, 2008; Wu *et al.*, 2010; Jensen, 2010; Bamber, 2012; Jacob *et al.*, 2012; Schrama
52 *et al.*, 2014; Velicogna *et al.*, 2014], which results in about 7 *mSv* of additional freshwater
53 inflow (1 *mSv* = 1000 m^3/s). In case of the glaciers in Alaska, a mass loss rate of about
54 50 Gt/yr has been estimated [Arendt *et al.*, 2002; Tamisiea *et al.*, 2005; Luthcke *et al.*,
55 2008; Berthier *et al.*, 2010; Jacob *et al.*, 2012].

56 These losses of land ice mass induce a rise in global mean sea level, due to the addi-
57 tional freshwater mass. Furthermore, the mass redistribution leads to a change of the
58 geoid height and crustal deformation affecting regional sea level ([Farrell and Clark, 1976;
59 Francis and Mazzege, 1990; Mitrovica *et al.*, 2001] and others). Moreover, regional sea
60 level is influenced by the freshening of seawater in the vicinity of the source region of the
61 freshwater. It reduces the density and increases the specific volume, resulting in regional
62 sea level rise. In addition to that, regional sea level responds to freshwater inflow due to
63 changes in ocean circulation. As is done in this study, these dynamic sea level changes
64 can be simulated using ocean models.

65 Several oceans model studies have been performed based on a variety of mass loss sce-
66 narios. An example is presented by Gerdes *et al.* [2006], who have analyzed the change of
67 dynamic sea level change from Greenland ice mass loss by changing the surface boundary

68 conditions in ocean general circulation models. The additional freshwater was converted
69 into additional rain and spread along the coasts of Greenland. This technique is generally
70 denoted as 'hosing'. *Gerdes et al.* [2006] found a reduced convection in the Labrador Sea.
71 In addition, the weakened deep western boundary current transported more saline water.
72 The study showed a strong sensitivity of the model results to the choice of the differ-
73 ent boundary conditions. They also identified uncertainties resulting from the missing
74 atmospheric response in ocean-only models.

75 When ocean circulation changes, oceanic temperature is advected differently. Thus the
76 air-sea temperature difference is altered affecting surface heat fluxes. The atmospheric
77 feedbacks, indirectly induced by continental ice mass loss and the associated variations at
78 the ocean's surface, have been studied using a coupled atmosphere-ocean models. *Stam-*
79 *mer et al.* [2011] compared the response of the ocean computed with an ocean-only model
80 [*Stammer, 2008*] and a coupled model. They investigated the response to Greenland Ice
81 Sheet mass loss during a 50-year simulation period and in the coupled model they found
82 the existence of far field signals in the Indian and Pacific Ocean, which have not been
83 visible in previous studies (e.g. *Gerdes et al., 2006*).

84 *Weijer et al.* [2012] showed that the spatial resolution is important when simulating
85 the freshwater transport in the ocean. For example, they identified an increase in the
86 velocity of the freshwater transport in the North Atlantic when using an eddy resolving
87 ocean model.

88 *Wang et al.* [2012] investigated the future ocean response to mass loss of the Greenland
89 Ice Sheet in a water hosing experiment using the FESOM model. They simulated sea
90 level and ocean circulation changes that are caused by a discharge rate of 0.1 Sv over 120

91 model years. Their results concentrate mainly on the consequences to meridional heat
92 transport and vertical overturning caused by additional freshwater fluxes. They found a
93 weakening of the AMOC strength and of its decadal variability.

94 *Brunnabend et al.* [2012] investigated the response of ocean circulation and the steric
95 contribution to the regional sea level caused by mass loss of the Greenland Ice Sheet
96 using the FESOM model. In that study, the associated steric contribution had only a
97 small influence on global mean sea level rise, as shown before by *Munk* [2003] and *Lowe*
98 *and Gregory* [2006]. On the other hand, the steric contribution led to strong regional
99 deviations. A pattern was identified in the North Atlantic, which changed over time
100 as the freshwater was distributed over the North Atlantic and the Arctic Ocean after 50
101 model years. The amount of the additional freshwater inflow around Greenland influenced
102 the amplitude of the signal. However, it had only a small influence on the structure of
103 the pattern, which may change when the additional mass loss would become high enough
104 to alter the ocean circulation pattern [*Brunnabend et al.*, 2014].

105 The response to uplift and geoid change, including rotational feedback effects, caused by
106 mass redistribution (in the following denoted as the static-equilibrium sea level response)
107 was investigated in a water hosing experiment by [*Kopp et al.*, 2010] in addition to the sea
108 level response due to the freshening and the changes in ocean circulation. A Greenland
109 ice mass loss of 0.1 Sv was uniformly added to ocean surface in the North Atlantic. They
110 found that dynamic sea level change has become significant at mass loss rates stronger than
111 detected currently. Static-equilibrium sea level change becomes dominant in most ocean
112 regions, except for the western North Atlantic, where freshwater contribution exceeded
113 about 20cm equivalent sea level.

114 While most hosing experiments apply high mass loss rates (e.g. 0.1 Sv) around Green-
115 land, this study applies mass loss rates that are representative for the last decade (i.e. 7
116 mSv or 200 Gt/yr) in the simulation experiments using a global configuration of the finite
117 element sea-ice ocean model (FESOM, *Wang et al.*, 2014; *Brunnabend et al.*, 2011). Here,
118 in addition to the investigation of the sea level response to the mass loss of the Greenland
119 Ice Sheet, we also investigate the sea level response to the mass loss of the West Antarctic
120 Ice Sheet and the glaciers in Alaska. The mass loss rates are assumed to be constant over
121 time and are included during predefined mass loss seasons in the model simulations. The
122 simulations are performed by applying each source of freshwater separately and in their
123 combination. In addition, sea level change due to variations in gravitational attraction
124 and the ocean floor deformation corresponding to ice mass loss, as well as the rotational
125 effects of the mass redistribution are estimated and added to the modeled dynamic sea
126 level change.

2. Data and Methods

2.1. Model Setup and Experiments

127 Monthly mean dynamic sea level change is calculated using the finite element sea-
128 ice ocean model FESOM [*Wang et al.*, 2014; *Brunnabend et al.*, 2011]. The model is
129 discretized on a global tetrahedral grid using the same mesh as applied in the study of
130 *Sidorenko et al.* [2011], i.e. an unstructured and rotated mesh where the poles are located
131 on land (Greenland and Antarctica). The model applies the set of primitive equations for
132 oceanic motion including a fully nonlinear free surface.. The horizontal resolution ranges
133 from 20 km near the coast and around Greenland to approximately 150 km in the open
134 ocean. The high horizontal resolution resolves the boundary currents, which are important

135 for the modeling of the freshwater transport. The vertical discretization is performed on
136 39 z-levels of varying thickness. The model does not account for ocean tides. Instead, it
137 includes M2 tidal mixing formulation derived from the tpxo07 tide model of *Egbert and*
138 *Erofeeva* [2002]. FESOM is initialized by using the temperature and salinity data of the
139 World Ocean Atlas (WOA01 *Stephens et al.* [2002]) and has a spin-up time period of 52
140 years (1958-2010) using NCEP forcing. The model is then run for one repeated period of
141 50 years (1960-2010), which defines the time period of the reference simulation as well as
142 of the simulations that include additional freshwater inflows. A time step of 45 minutes
143 is used.

144 The simulations performed in this study are forced with atmospheric datasets from
145 the daily NCAR/NCEP reanalysis [*Kalnay et al.*, 1996]. The global mean ocean mass
146 variations are directly linked to the freshwater fluxes from precipitation and evaporation
147 prescribed by the NCAR/NCEP reanalysis and to the daily river runoff, provided by the
148 land surface discharge model (LSDM, *Dill*, 2008). The freshwater flux is modeled as a flux
149 of volume and mass but not of salt. Heat fluxes are calculated with bulk formulae [*Wang*
150 *et al.*, 2014; *Timmermann et al.*, 2009] using daily mean shortwave and longwave radiation
151 flux, 2m temperature and 2m specific humidity of NCAR/NCEP reanalysis [*Kalnay et al.*,
152 1996]. No salinity or temperature restoring is used. The model applies the Boussinesq
153 approximation, which conserves volume rather than mass. Hence, a sea level adjustment
154 after *Greatbatch* [*Greatbatch*, 1994] is implemented to ensure conservation of mass.

155 Thermo-steric expansion and halo-steric contraction (steric height change) are ac-
156 counted for by using the equation of state of *Jackett and McDougall* [1995] and added
157 to modeled sea level change within the ocean model. However, modeled global mean

158 thermosteric expansion amounts to about 1.2 mm/year during the period 1970-2010 and
159 approximately 2 mm/year after 1993. These values are larger than the estimates of IPCC
160 AR5 which are 0.8 and 1.1mm/year, respectively [*Church et al.*, 2013].

161 In this study, five experiments have been performed that differ from the reference run
162 only by the additional input of freshwater, which is constant during the whole simulation
163 period of 50 years (table 1): (1) 200 Gt/yr of ice mass loss are converted to a volume
164 flux and then equally distributed to all nodes along the coast of Greenland, which are
165 located south of 75 degree north. (2) A freshwater inflow is included at the coast of the
166 Gulf of Alaska corresponding to an ice mass loss of 50 Gt/yr. The changes in mass of
167 all other mountain glaciers are not taken into account during this study as they are less
168 localized. (3) A freshwater inflow equal to 100 Gt/yr of ice mass loss is applied to the
169 West Antarctic coast. (4) The three mass loss scenarios described above are combined in
170 a model simulation, to investigate the linearity of regional sea level change caused by the
171 different contributions. For the same reason, (5) the mass losses of only the Greenland
172 and West Antarctic Ice Sheet are combined in a model simulation. In all simulations it is
173 assumed that for the northern hemisphere, freshwater inflow occurs from May to October
174 and for the southern hemisphere from November to April. Changes in regional sea level
175 are then computed by taking the difference between the reference model simulation and
176 the respective simulation including additional freshwater inflow.

2.2. Static-Equilibrium Sea Level Change

177 The reduced ice masses in Greenland, the West Antarctic and Alaska cause time-variable
178 differences of the geoid, including rotational effects, minus the uplift of the ocean bottom.
179 The sea level changes arising from the changing ice and ocean loads are computed using the

180 sea level equation, which is solved in spectral domain using real-valued fully normalized
181 spherical harmonic base functions [*Farrell and Clark, 1976; Rietbroek et al., 2012*]. The
182 unknown relative sea level is assumed to coincide with an equipotential surface, i.e. it
183 is responds to the gravitational effects of the prescribed load on land, the associated
184 rotational potential change, and the gravitational effects of the sea level itself [*Rietbroek*
185 *et al., 2012*]. The redistribution of mass between land ice and ocean, and within the
186 ocean, leads to a small shift of the Earth’s rotation axis. This leads to small changes
187 in centrifugal potential that, in turn, create a small but large-scale change in sea level.
188 When solving for the static equilibrium response, we use loading Love numbers from the
189 PREM Earth model [*Dziewonski, 1981*] to model the Earth’s deformation response to
190 surface loading, and the associated geoid response.

191 The linear behaviour of the sea level equation allows to superimpose the sea level contri-
192 butions from the major ice sheets and Alaskan glaciers. Therefore, to the mass loss of the
193 major ice sheet and the Alaska Glaciers, which are constructed for signals representative
194 for the last decade. Here, a time-invariant ocean function is assumed as it is expected that
195 the shoreline has not migrated by much during the time period of study. The patterns of
196 the mass loss regions are taken from the database of *Rietbroek et al. [2012]*, where the ice
197 mass loss in Greenland is assumed as to be uniform over the entire Greenland Ice Sheet.
198 The ice mass loss of the West Antarctic Ice Sheet is assumed to be uniform over the entire
199 West Antarctic excluding the Antarctic Peninsula. The self consistent sea level response
200 to melting of the Alaskan glaciers is taken from *Rietbroek et al. [2012]*.

201 In this study, the global mean sea level change has been subtracted from the static-
202 equilibrium sea level change as it is already contained in the mass conserving ocean model.
203 For more detailed information about the method, please refer to *Rietbroek et al.* [2012].

3. Results

3.1. Freshwater Distribution

204 The inflow of the additional freshwater is modeled as a flux of volume and mass which
205 leads to a non-linear response according to the equation of state for sea water. To study
206 the path of the freshwater a passive tracer is added to the inflow. This tracer is advected
207 by the ocean dynamics in the same way as temperature and salinity (which are not passive
208 tracers). The tracer distribution depicts the freshening of the ocean that is caused by the
209 mass loss of the ice sheets. Figure 1 shows the freshwater distribution that originates from
210 the West Antarctic Ice Sheet. The freshwater mainly stays in the region of the source,
211 however, as soon as it reaches the Antarctic Circumpolar Current (ACC) it is distributed
212 around the whole Antarctic continent. In addition, some freshwater flows west with the
213 coastal current. After reaching the Ross Sea Gyre, most of it sinks into the deeper ocean.
214 This water is subsequently distributed around the Antarctic continent at depth. Near the
215 surface, some freshwater passes the ACC and is transported through surface currents to
216 the north.

217 Figure 2 (a,b) shows the modeled passive tracer caused by the additional freshwater in-
218 flow near the coast of Greenland. These values describe the distribution of the freshwater
219 leading to halo-steric sea level rise. After 50 years (mean of year 50), the surface currents
220 have transported the freshwater from Baffin Bay and the Labrador Sea southward along
221 the North American coast, leaving some freshwater in Hudson Bay. Another part is trans-

ported via the sub-polar gyre to the European coast where it separates into two branches
flowing into the Arctic Ocean and along the sub-tropical gyre to the equatorial Atlantic
Ocean. Some freshwater is also sinking to greater depths where it spreads southward
along the American coast towards the South Atlantic Ocean. These results agree well
with studies from *Gerdes et al.* [2006] and *Brunnabend et al.* [2012].

Figure 2 (c,d) shows the passive tracer of the reduced salinity caused by freshwater
inflow from the Glaciers of Alaska. In this experiment, the freshwater is transported close
to the surface to the Arctic Ocean through Bering Strait where it flows into the Beaufort
Gyre and further into the North Atlantic Ocean. Only a small amount of freshwater is
transported southward near the eastern coast of North America to equatorial regions. In
addition, a small portion of the freshwater is directed to the equatorial Pacific Ocean.

3.2. Atlantic meridional overturning

The applied freshwater inflows caused by the mass loss of land ice have only small influ-
ence on the Atlantic meridional overturning circulation (AMOC). The maximum AMOC
at 45N is commonly used as an index to characterize the full overturning circulation. In
the reference simulation, the mean strength of the yearly mean AMOC at 45N is about
14.5 Sv ($1\text{Sv} = 10^6\text{m}^3/\text{s}$) with a variance of 3.1 Sv (figure 3a). Only the results of the ex-
periments, where the freshwater inflow of 200 Gt/yr around Greenland is included, show
a significant difference (experiments 1,4, and 5). A reduced salinity is slightly stabilizing
the water column in the region of deep water formation. The AMOC slows down. Its
maximum strength at 45N slowly decreases by about 1 Sv with respect to the reference
simulation within the first 30 years of the hosing period. Subsequently it remains at
the lower level with increased inter-annual variability (from 0.1 Sv to about 0.3 Sv). In

244 the experiments including only freshwater inflow caused by the ice mass loss of the West
245 Antarctic Ice Sheet or the glaciers in Alaska (experiment 2 and 3), the AMOC experiences
246 almost no change as the amount of freshwater reaching the deep water formation areas
247 is too small to initiate alterations in the water column. The AMOC remains at the same
248 level as the reference simulation (figure 3b). The difference with respect to the reference
249 simulation only slightly varies by about 0.06 Sv.

250 However, the modeled AMOC results strongly depend on the model configuration. The
251 strength of the AMOC is strongly influenced by the model parameterization and the
252 spatial resolution used during the model experiments. In the study of *Brunnabend et al.*
253 [2012], using a low resolution model grid (1.5 x 1.5 degrees), the AMOC was fairly weak
254 and more freshwater could reach the equatorial Atlantic Ocean. In the present study
255 however, the AMOC is stronger and the freshwater spreads out more in the direction
256 of the Arctic Ocean. Higher values (about 20 Sv at 45N) are reached in the study of
257 *Sidorenko et al.* [2009]. They used the finite-element ocean circulation model (FEOM)
258 with a horizontal resolution ranging from 0.2 to 1 degree in the North Atlantic with
259 highest resolution in the Gulf Stream area. Another difference to the model used here
260 is that temperature and salinity are forced by relaxation to monthly mean sea surface
261 temperature of the WOA01 climatology. Such a restoring is not applied here, as it would
262 distort the results of the hosing experiments.

3.3. Sea Level Change Caused by Land Ice Mass Loss

263 Beside the modeled global mean sea level change of about 0.6 mm/yr for a mass loss
264 rate of 200 Gt/yr, mainly the steric contribution in the ocean leads to regional sea level
265 change in the hosing experiments. Ocean circulation changes, caused by the applied mass

266 loss rates, appear to be rather small. However, this may change with increasing land
267 ice mass loss as for example stated by *Gregory et al.* [2003]; *Stammer* [2008]; *Stammer*
268 *et al.* [2011]; *Brunnabend et al.* [2014]. Modeled sea level change that is induced by the
269 land ice mass loss can be separated into its mass and steric contribution. After 50 years,
270 the pattern of sea level change is partly associated to the small reduction of the AMOC
271 [*Yin et al.*, 2009, 2010; *Kienert and Rahmstorf*, 2012], which causes a sea level rise at
272 the northeast American coast due to redistribution of ocean mass (figure 4a). The steric
273 contribution (figure 4b) is responsible for the complex pattern in the North Atlantic and
274 Arctic Ocean caused by the additional freshwater and an atmospheric feedback changing
275 the net heat flux between atmosphere and ocean.

276 Figure 5 shows the contributions to regional deviations from modeled global mean sea
277 level of the different regions of ice mass loss. After 50 years, variations in modeled sea level
278 are concentrated in the regions of freshwater inflow. In response to a Greenland Ice Sheet
279 mass loss of 200 Gt/yr (figure 5a and 5b), there are deviations from modeled global mean
280 sea level visible which are mainly located in the North Atlantic and the Arctic Ocean
281 (figure 5a). The process of how the modeled sea level changes within FESOM under a
282 Greenland mass loss scenario, is described in detail in the water-hosing experiment of
283 *Wang et al.* [2012].

284 The freshwater distribution, resulting from the freshwater inflow in Alaska, also leads
285 to a regional pattern of modeled sea level change in the North Atlantic Ocean (figure 5c
286 and 5d). But in contrast to the simulation including mass loss of the Greenland Ice Sheet,
287 modeled sea level rise in the Arctic is located mainly in shallow regions north of Alaska

288 and Canada corresponding to the flow path of the freshwater. In addition, the freshwater
289 tongue in the equatorial Pacific does not lead to a clear signal in modeled sea level change.

290 As most freshwater remains in the Southern Ocean in the West Antarctic ice mass loss
291 scenario, modeled sea level changes mainly occur in this region (figure 5e and 5f). The
292 modeled sea level rise near the source of ice mass loss is not as pronounced as in the
293 Greenland hosing experiment, as only half as much ice mass is lost and its is redistributed
294 to a larger area in the Southern Ocean by the ACC. However, far field variations are also
295 visible, e.g. in the North Atlantic (figure 5e). These are caused by changes in the heat
296 fluxes between atmosphere and ocean (not shown). Similar changes can be identified in
297 the two experiments including the Alaska and Greenland mass loss scenario.

298 Figure 6a shows the modeled sea level change due to the combined mass loss of the
299 two ice sheets and the glaciers of Alaska after 50 years including modeled global mean
300 sea level change. Strong sea level change is found near the coast where the ice mass is
301 lost. This especially holds for the Greenland coast where most freshwater flows into the
302 ocean. The corresponding static-equilibrium sea level change (figure 6b) decreases in the
303 vicinity of the sources and slightly increases at greater distances. As pointed out by earlier
304 studies (e.g. *Mitrovica et al.* [2001]), the decrease due to the static equilibrium change is
305 larger than the modeled increase in steric height and modeled sea level now falls in the
306 regions around Greenland. Near the coast of the West Antarctic Ice Sheet and the Alaska
307 Glaciers the sea level rise becomes lower than the global mean sea level change (Figure
308 6c).

309 One may wonder whether modeled sea level change of the simulation, including com-
310 bined mass losses, and the sum of the three simulations, which consider the mass contri-

311 butions separately, add up to the same effect. Figure 6d and 6e show that this is not the
312 case. Here, differences up to $\pm 3\text{cm}$ mainly occur in the North Atlantic and the Arctic
313 Ocean after 50 years. They arise as the different freshwater contributions interact with
314 each other in the simulation using the combined ice mass loss. These interactions are
315 not considered when simulating regional sea level change caused by the different sources
316 separately. Hence, ocean circulation may react differently causing local differences in sea
317 level. This also leads to different heat flux between atmosphere and ocean, mainly re-
318 sponsible for the difference in the North Atlantic. The effects due to this non-linearity
319 are generally smaller than the regional sea level change but are nonetheless visible and
320 therefore become important when investigating sea level change caused by land ice mass
321 loss.

322 Sea level change at a number of coastal locations around the North Atlantic Ocean are
323 chosen (figure 7) where the impact of ice mass loss appeared most significant. Figure
324 8a and 8b show the change in sea level at different location at European and the North
325 American coast, respectively. Signals from steric and mass contribution are separated.
326 Additionally, the static-equilibrium sea level change due to the land ice mass losses are
327 shown. At the European coast, sea level is mainly influenced by the additional mass.
328 The mass contribution in this coastal region is slightly higher than the global mean sea
329 level change due the additional freshwater. On the other hand, the steric contribution
330 is rather small. It is one order of magnitude smaller than the mass contribution. The
331 static-equilibrium sea level change compensates the extra mass contribution leading to a
332 regional sea level change lower than the global mean.

333 During the 50 years of the simulation experiments, sea level changes appears to be most
334 of the time of about 2cm above the global mean along the coast of Port-Aux-Basques,
335 Canada (Figure 8b). In this region, the modeled steric contribution becomes stronger
336 especially at the northern locations (e.g. at Port-Aux-Basques). Here the modeled steric
337 contribution reaches about one third of the amplitude of the mass contribution. The
338 modeled mass increase due to the change in circulation is also significant, outweighing
339 the signal of the static-equilibrium sea level change. Although these locations are fairly
340 close to the sources of the mass loss in Greenland, they are not near enough for this
341 signal to dominate regional sea level change in this simulation. These might change when
342 simulating with higher mass loss rates or applying a longer simulation time period.

4. Discussion and Conclusion

343 Besides the mass loss of the Greenland Ice Sheet this study also includes ice mass loss
344 of the West Antarctic Ice Sheet as well as the Alaskan Glaciers. It shows that rates of
345 ice mass loss, which are one order of magnitude smaller than in previous studies, lead to
346 a signal in regional deviations from modeled global mean sea level change in the order of
347 several centimeters. The land ice mass loss in different regions lead to different signals
348 in modeled regional sea level change with largest signals near its source. Here, the steric
349 signal is dominant and are caused by the additional freshwater, whereas during the 50
350 years of the model simulations changes circulation patterns are rather small. Only the
351 small reduction of the AMOC in the experiments including the mass loss of the Greenland
352 Ice Sheet leads to a redistribution of mass towards the coast mainly in the North Atlantic
353 and the Arctic Ocean.

354 Atmospheric feedbacks potentially play an important role in the North Atlantic since,
355 depending on the forcing parameters, the heat exchange between ocean and atmosphere
356 changes. *Stammer et al.* [2011] used a coupled model for simulating the ocean and atmo-
357 spheric response to Greenland ice mass loss. They showed that changing the freshwater
358 inflow around Greenland leads to atmospheric responses not only in regions where the ad-
359 ditional freshwater accumulates but also in far distant regions such as the Indian Ocean.
360 In addition, the strength of the AMOC is of major importance when simulating the merid-
361 ional heat transport. This heat transport reacts very sensitive to the changes in the AMOC
362 [*Stammer et al.*, 2011] and was reduced to a very low level. The results of *Stammer et al.*
363 [2011] indicate that also coupled models are very sensitive to their parameterization, and
364 that different models might react differently. For example, the model setup used in the
365 study of *Gerdes et al.* [2006] shows less impact. For these reason, it would be desirable
366 to have more sensitivity studies using coupled atmosphere-ocean models and uncoupled
367 ocean models. It should be noted that, for our study, atmospheric fields and fluxes from a
368 reanalysis are used, which include quite an amount of data assimilation. Therefore, most
369 of the real feedback of the atmosphere ocean system over the past 50 years is already
370 accounted for in our experiments.

371 Static-equilibrium sea level change caused by the redistribution of the ice mass may have
372 the same order of magnitude compared to the steric sea level response and the change
373 due to different ocean circulation. Our findings support the study of *Kopp et al.* [2010]
374 stating that the anomalies get locally dominant with higher mass loss rates. In addition,
375 this might be also true when investigating longer time series. The pattern of the static-
376 equilibrium sea level response remains constant over time. However, sea level changes due

377 to the response of freshwater inflow vary regionally and in time as ocean circulation may
378 change and the freshwater is transported to regions that are farther away from the origin
379 of the freshwater source.

380 Differences to reality may also be caused by our approximations of the melting rates
381 and locations in this study. Possibly, not as much ice mass was lost during the first
382 decades of the simulations as in the last decades [*Lemke et al.*, 2007] and recent ice mass
383 loss in Greenland is well above our applied rate [*Schrama et al.*, 2014]. Beside sediment
384 compaction and vertical land movement caused by earthquakes and/or local GIA, also the
385 contributions of the mountain glaciers and other hydrological sources are not accounted
386 for here.

387 To improve the current study, several advances can be made. Geodetic observations
388 of ice mass loss may be used as improved input parameters in the model. Furthermore,
389 the sea level contributions from mountain glaciers needs to be taken into account. In
390 possible future studies, modeled sea level change caused by ocean warming, including the
391 deep ocean, may be investigated. Also it is beneficial to increase the horizontal in the
392 open ocean, e.g. to model a more realistic AMOC that may change the dynamic sea level
393 response due to the additional freshwater as shown e.g. by Weijer et al. (2012).

394 **Acknowledgments.** The authors acknowledge support provided by the German Re-
395 search Foundation (DFG) under grants KU 1207/9-1 and SCHR779/6-1 within the Special
396 Priority Program SPP 1257 "Mass Transport and Mass Distribution in the System Earth".
397 We would like to thank the NOAA Climate Diagnostics Center, Boulder, for providing
398 the NCEP/NCAR reanalyzes online at <http://www.cdc.noaa.gov>. In addition, we would

399 like to thank Robert Dill for providing river runoff from the LSDM model. We thank
400 Dmitry Sidorenko for providing the script to compute the AMOC.

References

- 401 Arendt, A. A., K. A. Echelmeyer, W. D. Harrison, C. S. Lingle, and V. B. Valentine
402 (2002), Rapid Wastage of Alaska Glaciers and their Contribution to Rising Sea Level,
403 *Science*, *297*, 382–386.
- 404 Bamber, J. (2012), Shrinking glaciers under scrutiny, *Nature*, *482*, 482–483.
- 405 Berthier, E., E. Schiefer, G. K. C. Clarke, B. Menounos, and F. Remy (2010), Contribution
406 of Alaskan glaciers to sea-level rise derived from satellite imagery, *Nat. Geosci.*, *3*, 92–95,
407 doi: 10.1038/ngeo737.
- 408 Bindoff, N. L., J. Willebrand, V. Artale, C. A. J. Gregory, S. Gulev, K. Hanawa, C. L. Qiu,
409 S. Levitus, Y. Nojiri, C. K. Shum, L. D. Talley, and A. Unnikrishnan (2007), Obser-
410 vations: Oceanic Climate Change and Sea Level, in *The Scientific Basis, Contribution*
411 *of Working Group I to the Fourth Assessment Report of the Intergovernmental Panel*
412 *on Climate Change*, edited by S. Solomon, D. Qin, M. Manning, Z. Chen, M. Marquis,
413 K. B. Averyt, M. Tignor, and H. L. Miller, Cambridge University Press, Cambridge,
414 New York.
- 415 Brunnabend, S.-E., R. Rietbroek, R. Timmermann, J. Schröter, and J. Kusche (2011), Im-
416 proving mass redistribution estimates by modeling ocean bottom pressure uncertainties,
417 *J. Geophys. Res.*, *116*, C08037 doi: 10.1029/2010JC006617.
- 418 Brunnabend, S.-E., J. Schröter, R. Timmermann, R. Rietbroek, and J. Kusche (2012),
419 Modeled steric and mass-driven sea level change caused by Greenland Ice Sheet melting,

- 420 *J. Geodyn.*, doi: 10.1016/j.jog.2011.06.001.
- 421 Brunnabend, S.-E., H. A. Dijkstra, M. A. Kliphuis, B. van Werkhoven, H. E. Bal, F. Se-
422 instra, J. Maassen, and M. van Meersbergen (2014), Changes in extreme regional sea
423 surface height due to an abrupt weakening of the Atlantic meridional overturning cir-
424 culation, *Ocean Science*, *10*, 881–891, doi: 10.5194/os-10-881-2014.
- 425 Cazenave, A., A. Lombard, and W. Llovel (2008), Present-day sea level rise: A synthesis,
426 *Comptes Rendus Geoscience*, *340*, 761770, doi:10.1016/j.crte.2008.07.008.
- 427 Chen, J. L., C. R. Wilson, D. Blankenship, and B. Tapley (2009), Accelerated antarctic ice
428 loss from satellite gravity measurements, *Nat. Geosci.*, *2*, 859–862, doi:10.1038/ngeo694.
- 429 Church, J. A., and N. J. White (2011), Sea-Level Rise from the Late 19th to the Early
430 21st Century, *Surv. Geophys.*, *32*, 585602, doi: 10.1007/s10712-011-9119-1.
- 431 Church, J. A., P. Clark, A. Cazenave, J. Gregory, S. Jevrejeva, A. Levermann, M. Merri-
432 field, G. Milne, R. Nerem, P. Nunn, A. Payne, W. Pfeffer, D. Stammer, and A. Unnikr-
433 ishna (2013), Sea Level Change, in *The Scientific Basis, Contribution of Working Group*
434 *I to the Fifth Assessment Report of the Intergovernmental Panel on Climate Change*,
435 edited by T. F. Stocker, D. Qin, G.-K. Plattner, M. Tignor, S. K. Allen, J. Boschung,
436 A. Nauels, Y. Xia, V. Bex, and P. Midgley, Cambridge University Press, Cambridge,
437 United Kingdom and New York, NY, USA.
- 438 Dill, R. (2008), Hydrological model LSDM for operational earth rotation and gravity field
439 variations, *Scientific Technical Report; 08/09*, Helmholtz-Zentrum Potsdam Deutsches
440 GeoForschungsZentrum, *37*, doi: 10.2312/GFZ.b103-08095.
- 441 Dziewonski, A. (1981), Preliminary reference earth model, *Physics of The Earth and*
442 *Planetary Interiors*, *25 (4)*, 297–356, doi:10.1016/0031-9201(81)90046-7.

- 443 Egbert, G., and S. Erofeeva (2002), Efficient inverse modeling of barotropic ocean tides,
444 *J. Atmos. Oceanic Technol.*, *19*, 183–204.
- 445 Farrell, W. E., and J. A. Clark (1976), On Postglacial Sea Level, *Geophys. J. R. Astron.*
446 *Soc.*, *46*, 647–667.
- 447 Francis, O., and P. Mazzega (1990), Global charts of ocean tide loading effects, *J. Geophys.*
448 *Res.*, *95*, 411–424.
- 449 Gerdes, R., W. Hurlin, and S. M. Griffies (2006), Sensitivity of a global ocean model to
450 increased run-off from Greenland, *Ocean Model.*, *12*, doi: 10.1016/j.ocemod.2005.08.003.
- 451 Gouretski, V., and K. P. Koltermann (2007), How much is the ocean really warming,
452 *Geophys. Res. Lett.*, *34*, doi: L01610 10.1029/2006GL027834.
- 453 Greatbatch, R. J. (1994), A note on the representation of steric sea level in models that
454 conserve volume rather than mass, *J. Geophys. Res.*, *99*, 12,767–12,771.
- 455 Gregory, J. M., O. A. Saenko, and A. J. Weaver (2003), The role of the Atlantic freshwater
456 balance in the hysteresis of the meridional overturning circulation, *Climate Dynamics*,
457 *21*, 707–717, doi: 10.1007/s00382-003-0259-8.
- 458 Gregory, J. M., N. J. White, J. A. Church, M. F. P. Bierkens, J. E. Box, M. R. van den
459 Broeke, J. G. Cogley, X. Fettweis, E. Hanna, P. Huybrechts, L. F. Konikow, P. W.
460 Leclercq, B. Marzeion, J. Oerlemans, M. E. Tamisiea, Y. Wada, L. M. Wake, and
461 R. S. W. van de Wal (2013), Twentieth-Century Global-Mean Sea-Level Rise: Is the
462 Whole Greater than the Sum of the Parts?, *Journal of Climate*, *26*, 4476–4499, doi:
463 10.1175/JCLI-D-12-00319.1.
- 464 Gunter, B., T. Urban, R. Riva, M. Helsen, R. Harpold, S. Poole, P. Nagel, B. Schutz, and
465 B. Tapley (2009), A comparison of coincident GRACE and ICESat data over Antarctica,

- 466 *J. of Geod.*, *34*, 1051–1060, doi: 10.1007/s00190-009-0323-4.
- 467 Jackett, D., and T. J. McDougall (1995), Stabilization of hydrographic data, *Atmospheric*
468 *and Oceanic Technology*, *12*, 381–89.
- 469 Jacob, T., J. Wahr, W. T. Pfeffer, and S. Swenson (2012), Recent contribution of glaciers
470 and ice caps to sea level rise, *Nature*, *482*, 514–518, doi: 10.1038/nature10847.
- 471 Jensen, L. (2010), Schätzung der Eismassenbilanz von Grönland mit Hilfe von GRACE
472 und komplementären Daten, Master thesis, Universität Bonn, Germany.
- 473 Kalnay, E., M. Kanamitsu, R. Kistler, W. Collins, D. Deaven, L. Gandin, M. Iredell,
474 S. Saha, G. White, J. Woollen, Y. Zhu, M. Chelliah, W. Ebisuzaki, W. Higgins,
475 J. Janowiak, K. Mo, C. Ropelewski, J. Wang, A. Leetmaa, R. Reynolds, R. Jenne,
476 and D. Joseph (1996), The NCEP/NCAR 40-year reanalysis project, *Bull. Amer. Met.*
477 *Soc.*, *77*, 437–471.
- 478 Kienert, H., and S. Rahmstorf (2012), On the relation between Meridional Overturning
479 Circulation and sea-level gradients in the Atlantic, *Earth System Dynamics*, *3*, 109–120,
480 doi: 10.5194/esd-3-109-2012.
- 481 Kopp, R. E., J. X. Mitrovica, S. M. Griffies, J. Yin, C. C. Hay, and R. J. Stouffer (2010),
482 The impact of Greenland melt on local sea levels: a partially coupled analysis of dynamic
483 and static equilibrium effects in idealized water-hosing experiments, *Climate Change*,
484 *103*, 619–625, doi: 10.1007/s10584-010-9935-1.
- 485 Lemke, P., J. Ren, R. B. Alley, I. Allison, J. Carrasco, G. Flato, Y. Fujii, G. Kaser,
486 P. Mote, R. H. Thomas, and T. Zhang (2007), Observations: Changes in Snow, Ice and
487 Frozen Ground, in *Climate Change 2007: The Physical Science Basis. Contribution of*
488 *Working Group I to the Fourth Assessment Report of the Intergovernmental Panel on*

- 489 *Climate Change*, edited by S. Solomon, D. Qin, Z. C. M. Manning, M. Marquis, K. B.
490 Averyt, M. Tignor, and H. L. Miller, Cambridge University Press, Cambridge, New
491 York.
- 492 Levitus, S., J. I. Antonov, and T. P. Boyer (2005), Warming of the world ocean, 1995-2003,
493 *Geophys. Res. Lett.*, *32*, doi: L02604 10.1029/2004GL021592.
- 494 Lowe, J. A., and J. M. Gregory (2006), Understanding projections of sea level
495 rise in a Hadley Centre coupled climate model, *J. Geophys. Res.*, *11*, c11014,
496 doi:10.1029/2005JC003421.
- 497 Luthcke, S. B., H. J. Zwally, W. Abdalati, D. D. Rowlands, R. D. Ray, R. S. Nerem,
498 F. Lemoine, J. J. McCarthy, and D. S. Chinn (2006), Recent Greenland Ice Mass Loss
499 by Drainage System from Satellite Gravity Observations, *Science*, *314*, 1286–1289, doi:
500 10.1126/science.1130776.
- 501 Luthcke, S. B., A. A. Arendt, D. D. Rowlands, J. J. M. Carthy, and C. F. Larsen (2008),
502 Recent glacier mass changes in the gulf of alaska region from grace mascon solutions,
503 *J. Glaciol.*, *54*, 767–777.
- 504 Mitrovica, J. X., M. E. Tamisiea, J. L. Davis, and G. A. Milne (2001), Recent mass
505 balance of polar ice sheets inferred from patterns of global sea-level change, *Nature*,
506 *409*, 1026–1029.
- 507 Munk, W. (2003), Ocean Freshening, Sea Level Rising, *Science*, *300*, 2041–2043, doi:
508 10.1126/science.1085534.
- 509 Rietbroek, R., S.-E. Brunnabend, J. Kusche, and J. Schröter (2012), Resolving sea level
510 contributions by identifying fingerprints in time-variable gravity and altimetry, *Journal*
511 *of Geodynamics*, *59-60*, 72–81, doi: 10.1016/j.jog.2011.06.007.

- 512 Rignot, E., J. L. Bamber, M. R. van den Broeke, C. D. Y. Li, W. J. van de Berg, and
513 E. V. Meijgaard (2008), Recent Antarctic ice mass loss from radar interferometry and
514 regional climate modelling, *Nat. Geosci.*, *1*, doi:10.1038/ngeo102.
- 515 Schoen, N., A. Zammit-Mangion, J. C. Rougier, T. Flament, F. Remy, S. Luthcke, and
516 J. L. Bamber (2015), Simultaneous solution for mass trends on the West Antarctic Ice
517 Sheet, *The Cryosphere*, *9*, 805–819, doi:10.5194/tc-9-805-2015.
- 518 Schrama, E., B. Wouters, and R. Rietbroek (2014), A mascon approach to assess ice
519 sheet and glacier mass balances and their uncertainties from GRACE data., *Journal of*
520 *Geophysical Research: Solid Earth*, *119*, 6048–6066, doi: 10.1002/2013JB010923.
- 521 Sidorenko, D., S. Danilov, Q. Wang, A. Huerta-Casas, and J. Schröter (2009), On
522 computing transports in finite-element models, *Ocean Modelling*, *28* (1), 60–65,
523 doi:10.1016/j.ocemod.2008.09.001.
- 524 Sidorenko, D., Q. Wang, S. Danilov, and J. Schröter (2011), FESOM under coordinated
525 ocean-ice reference experiment forcing, *Ocean Dyn.*, *61*, 881–890, doi:10.1007/s10236-
526 011-0406-7.
- 527 Stammer, D. (2008), Response of the global ocean to Greenland and Antarctic ice melting,
528 *J. Geophys. Res.*, *113*, C06022, doi: 10.1029/2006JC004079.
- 529 Stammer, D., N. Agarwal, P. Herrmann, A. Köhl, and C. R. Mechoso (2011), Response
530 of a Coupled Ocean-Atmosphere Model to Greenland Ice Melting, *Surv. Geophys.*, *32*,
531 621–642, doi: 10.1007/s10712-011-9142-2.
- 532 Stephens, C., J. I. Antonov, T. P. Boyer, M. E. Conkright, R. Locarnini, and T. D.
533 O’Brien (2002), *World Ocean Atlas 2001*, NOAA Atlas NESDID 49, US Govt. Printing
534 Office, Washington, DC.

- 535 Tamisiea, M. E., E. W. Leuliette, J. L. Davis, and J. X. Mitrovica (2005), Constraining
536 hydrological and cryospheric mass flux in southeastern Alaska using space-based gravity
537 measurements, *Geophys. Res. Lett.*, *32*, L20501 doi:10.1029/2005GL023961.
- 538 Timmermann, R., S. Danilov, J. Schröter, C. Böning, D. Sidorenko, and K. Rollenhagen
539 (2009), Ocean circulation and sea ice distribution in a finite-element global sea ice -
540 ocean model, *Ocean Model.*, *27*, 114–129, doi: 10.1016/j.ocemod.2008.10.009.
- 541 van der Wal, W., P. L. Whitehouse, and E. J. Schrama (2015), Effect of GIA models with
542 3D composite mantle viscosity on GRACE mass balance estimates for Antarctica, *Earth
543 and Planetary Science Letters, Elsevier*, *414*, 134–143, doi:10.1016/j.epsl.2015.01.001.
- 544 Vaughan, D., J. Comiso, I. Allison, J. Carrasco, G. Kaser, R. Kwok, P. Mote, T. Murray,
545 F. Paul, J. Ren, E. Rignot, O. Solomina, K. Steffen, and T. Zhang (2013), Observa-
546 tions: Cryosphere, in *Climate Change 2013: The Physical Science Basis. Contribution
547 of Working Group I to the Fifth Assessment Report of the Intergovernmental Panel on
548 Climate Change*, edited by T. Stocker, D. Qin, G.-K. Plattner, M. Tignor, S. Allen,
549 J. Boschung, A. Nauels, Y. Xia, V. Bex, and P. Midgley, Cambridge University Press,
550 Cambridge, United Kingdom and New York, NY, USA.
- 551 Velicogna, I., T. C. Sutterley, and M. R. van den Broeke (2014), Regional acceleration in
552 ice mass loss from Greenland and Antarctica using GRACE time-variable gravity data,
553 *Geophys. Res. Lett.*, *41*, doi: 10.1002/2014GL061052.
- 554 Wang, Q., S. Danilov, D. Sidorenko, R. Timmermann, C. Wekerle, X. Wang, T. Jung,
555 and J. Schröter (2014), The Finite Element Sea Ice-Ocean Model (FESOM) v.1.4: for-
556 mulation of an ocean general circulation model, *Geosci. Model Dev.*, *7* (2), 663–693,
557 doi:10.5194/gmd-7-663-2014.

- 558 Wang, X., Q. Wang, D. Sidorenko, S. Danilov, J. Schröter, and T. Jung (2012), Long
559 term ocean simulations in FESOM: Validation and application in studying the impact
560 of Greenland Ice Sheet melting, *Ocean Dyn.*, doi: 10.1007/s10236-012-0572-2.
- 561 Weijer, W., M. E. Maltrud, M. W. Hecht, H. A. Dijkstra, and M. A. Kliphuis (2012),
562 Response of the Atlantic Ocean circulation to Greenland Ice Sheet melting in a strongly-
563 eddying ocean model, *Geophys. Res. Lett.*, *39*, L09606, doi: 1029/2012GL051611.
- 564 Whitehouse, P. L., M. J. Bentley, G. A. Milne, M. A. King, and I. D. Thomas (2012),
565 A new glacial isostatic adjustment model for Antarctica: calibrated and tested using
566 observations of relative sea-level change and present-day uplift rates, *Geophys. J. Int.*,
567 *190*, 14641482, doi: 10.1111/j.1365-246X.2012.05557.x.
- 568 Williams, S. D. P., P. Moore, M. A. King, and P. L. Whitehouse (2014), Revisiting
569 GRACE Antarctic ice mass trends and accelerations considering autocorrelation, *Earth
570 and Planetary Science Letters*, *385*, 12–21, doi: 10.1016/j.epsl.2013.10.016.
- 571 Wouters, B., D. Chambers, and E. J. O. Schrama (2008), GRACE observes small-scale
572 mass loss in Greenland, *Geophys. Res. Lett.*, *35*, L20501, doi: 10.1029/2008GL034816.
- 573 Wu, X., M. B. Heflin, H. Schotman, B. L. A. Vermeersen, D. Dong, R. S. Gross, E. R.
574 Ivins, A. W. Moore, and S. E. Owen (2010), Simultaneous estimation of global present-
575 day water transport and glacial isostatic adjustment, *Nat. Geosci.*, *3*, 642–646, doi:
576 10.1038/ngeo938.
- 577 Yin, J., M. E. Schlesinger, and R. J. Stouffer (2009), Model projections of rapid sea-
578 level rise on the northeast coast of the United States, *Nat. Geosci.*, *2*, 262–266, doi:
579 10.1038/ngeo462.

Figure 1. Passive tracer corresponding to the reduced salinity (in psu), depicting the distribution of the freshwater inflow from the West Antarctic Ice Sheet at different depth (after 50 years): (a,c) surface, (b,d) 1500 m. Note the different color scale of the different panels (a and b vs. c and d) to show the signals in the Southern Ocean and the North Atlantic.

Figure 2. Passive tracer corresponding to the reduced salinity (in psu), depicting the distribution of the freshwater inflow along the coast of Greenland (a,b), and the Alaska Glaciers (c,d) at different depth (after 50 years): (a,c) surface, (b,d) 1500 m. Note the different color scale of the different panels.

Figure 3. Maximum AMOC at 45N of (a) the control simulation and (b) the response to the additional freshwater inflow of the different experiments

Figure 4. Modeled regional sea level change due to ice mass loss in meters after 50 years including all mass loss locations in the model simulation, separated into (a) ocean mass redistribution, where the global mean change of 5.1cm is subtracted and (b) steric height change.

Figure 5. Regional deviations from global mean sea level in meter after 50 years caused by mass loss of the major ice sheets and glaciers in Alaska: (global and polar projection) (a) and (b) deviation from global mean sea surface height change in case of mass loss of the Greenland Ice Sheet (200 Gt/yr); (c) and (d) deviation from global mean sea surface height change in case of mass loss of change the Alaska Glaciers (50 Gt/yr); (e) and (f) deviation from global mean sea surface height change in case of mass loss of the West Antarctic Ice Sheet (100 Gt/yr).

580 Yin, J., S. M. Griffies, and R. J. Stouffer (2010), Spatial Variability of Sea Level
581 Rise in Twenty-First Century Projections, *Journal of Climate*, 23, 4585–4607, doi:
582 10.1175/2010JCLI3533.1.

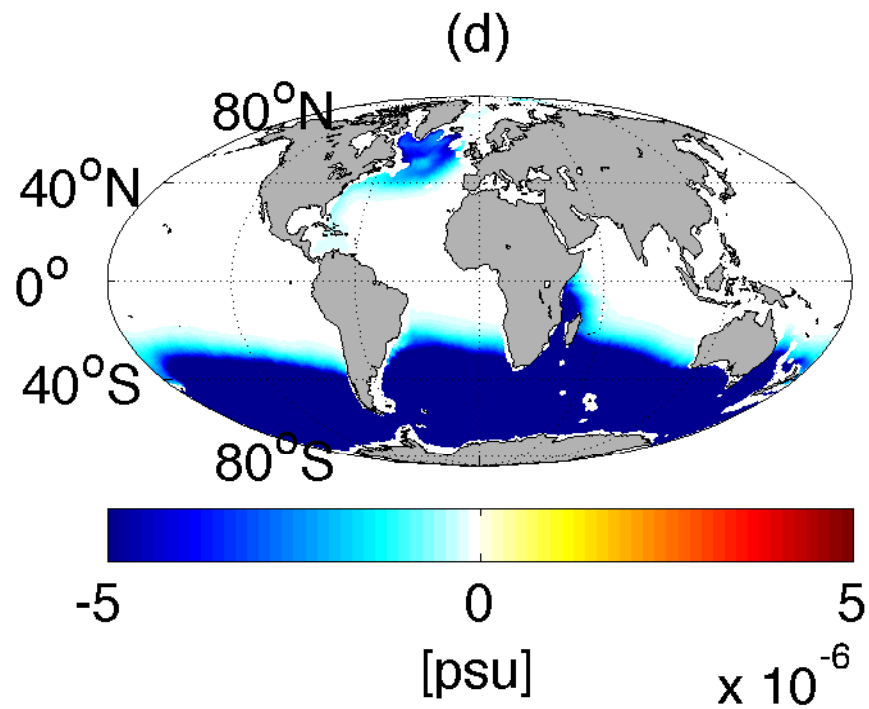
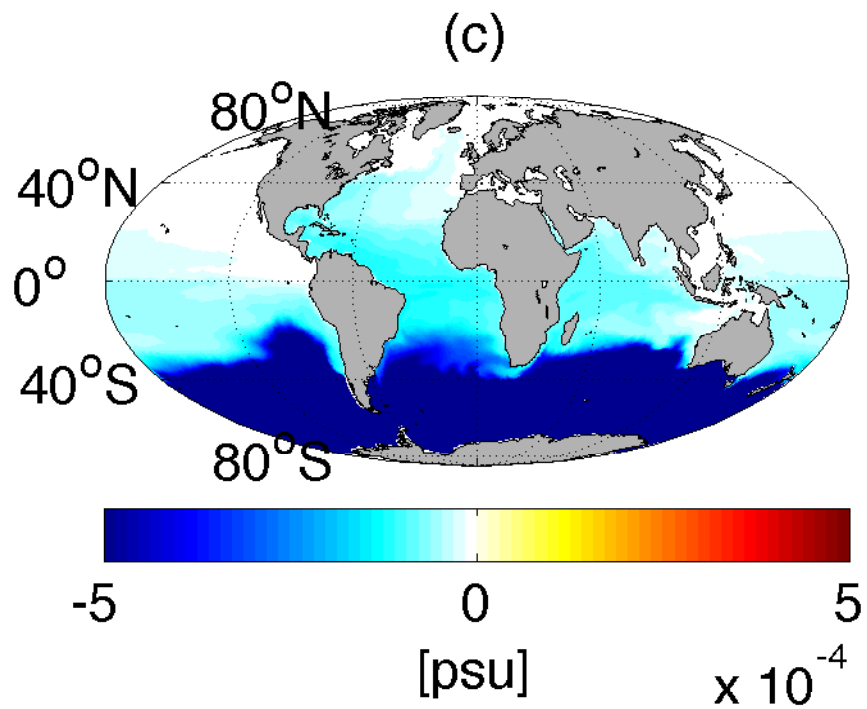
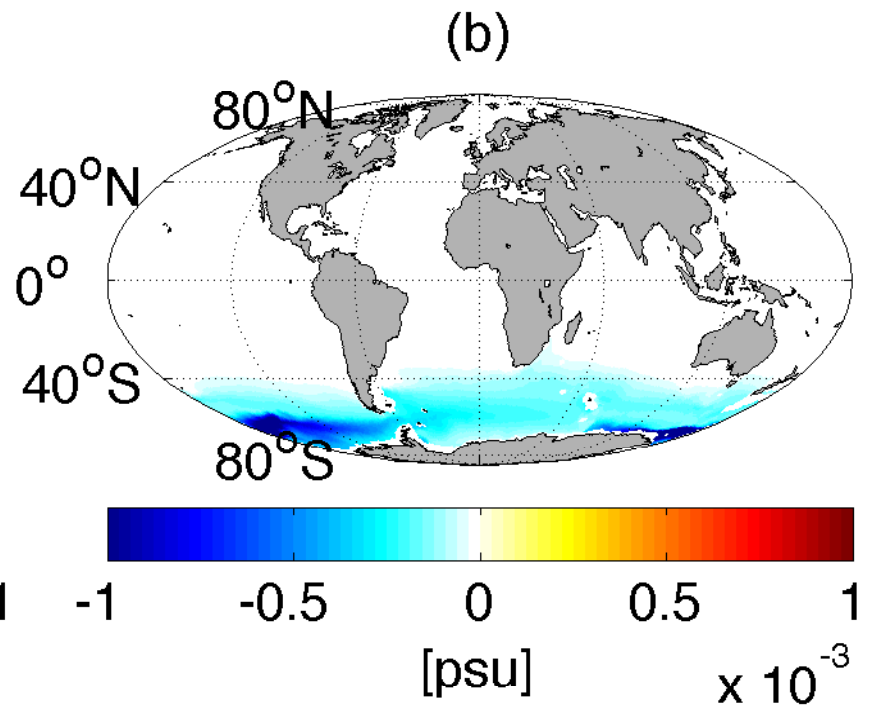
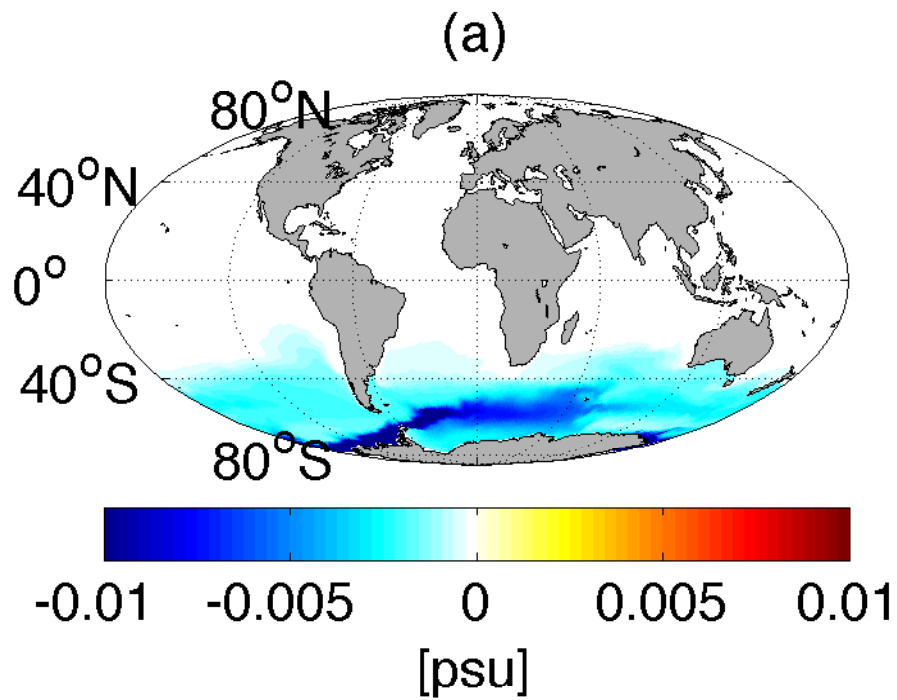
Figure 6. Regional sea level change caused by mass loss of the major ice sheets and the Alaska Glaciers (after 50 years in meter): (a) modeled sea level change, including the mass loss in all three regions; (b) static-equilibrium sea level change; (c) regional sea level change (a+b); (d) difference between modeled sea level change of the simulation considering the three contributors (shown in figure a) and sea level change computed as sum of the three simulations considering the sources of mass loss separately; (e) difference between modeled sea level change of the simulation considering the contributors from Greenland and the West Antarctic and sea level change computed as sum of these two simulations considering the sources of mass loss separately.

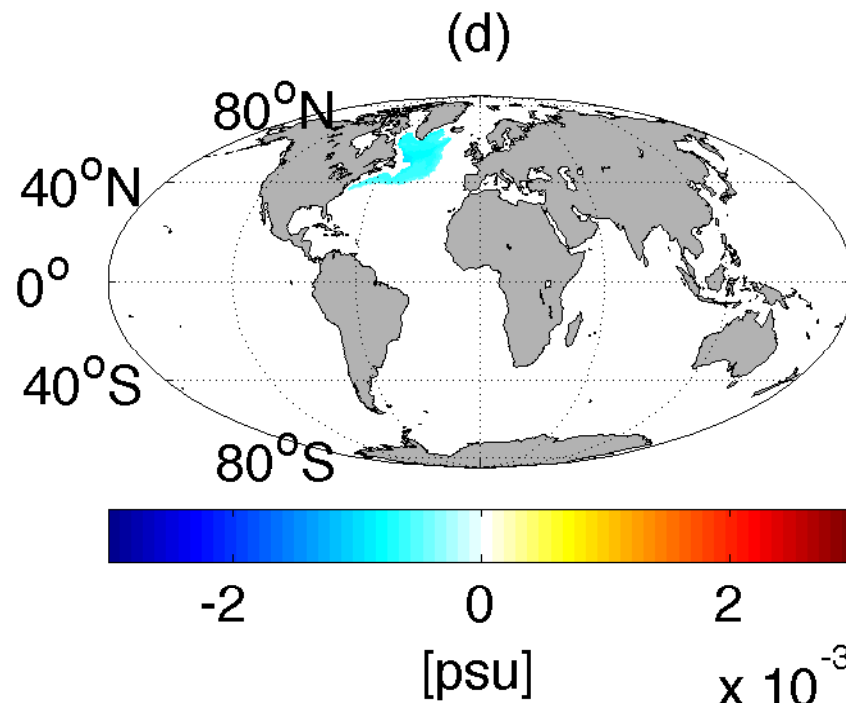
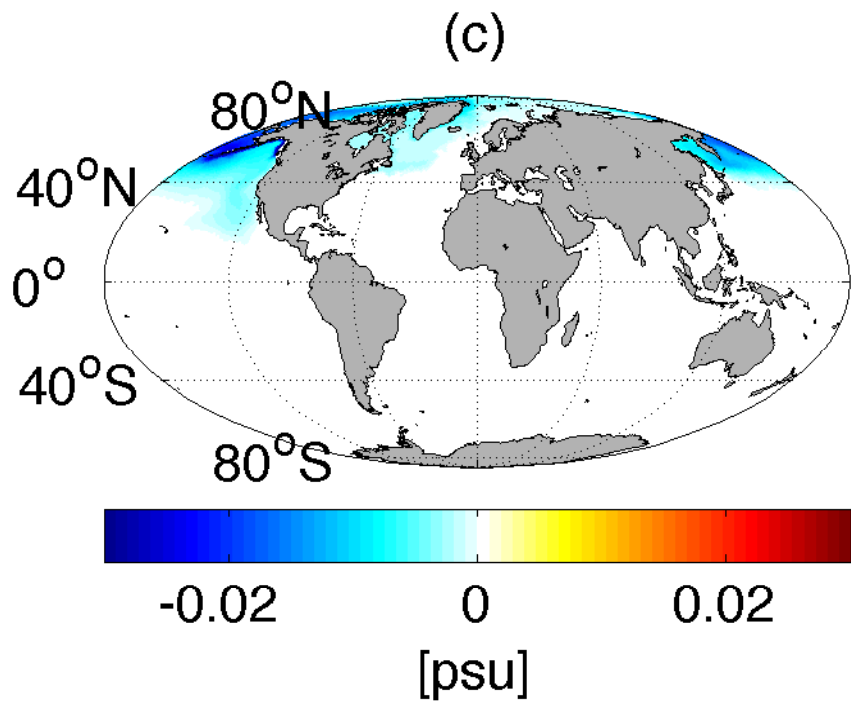
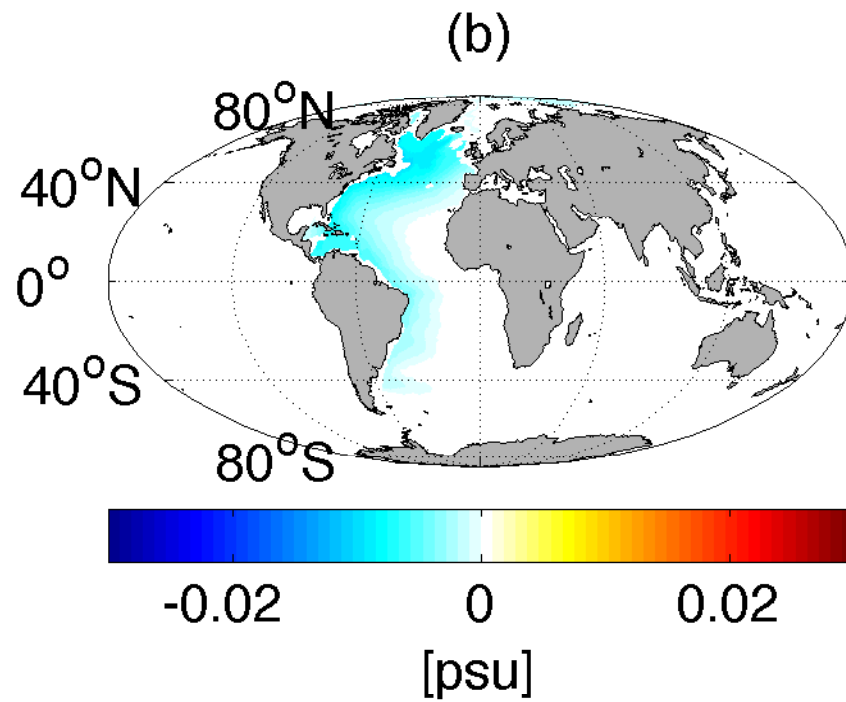
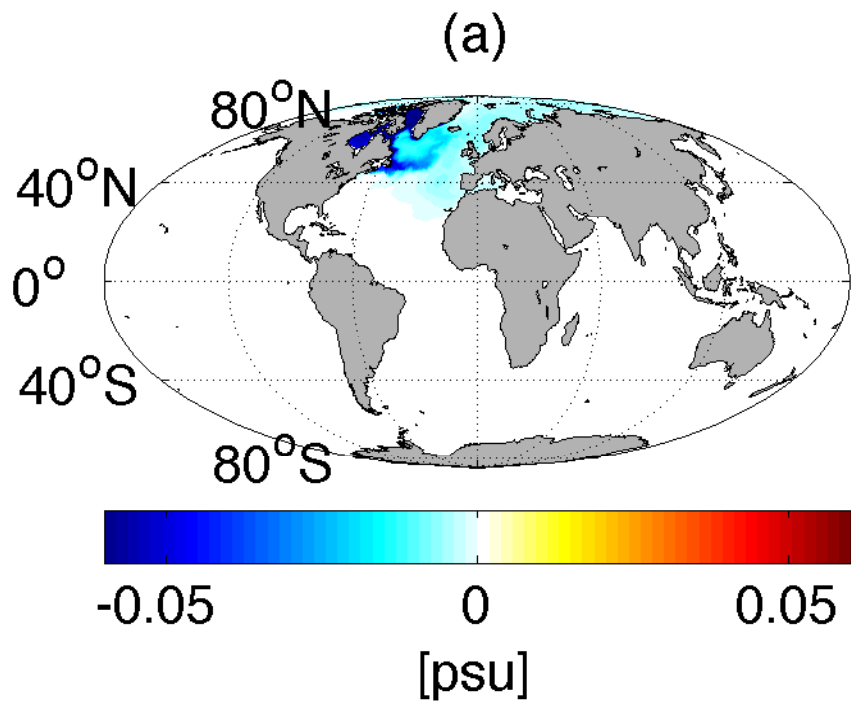
Figure 7. Locations at the North American and European coast.

Figure 8. Modeled mass and steric contributions to sea level change and the static equilibrium sea level change caused by land ice mass loss at different coastal locations in the North Atlantic region: (a) European coast (b) North American coast.

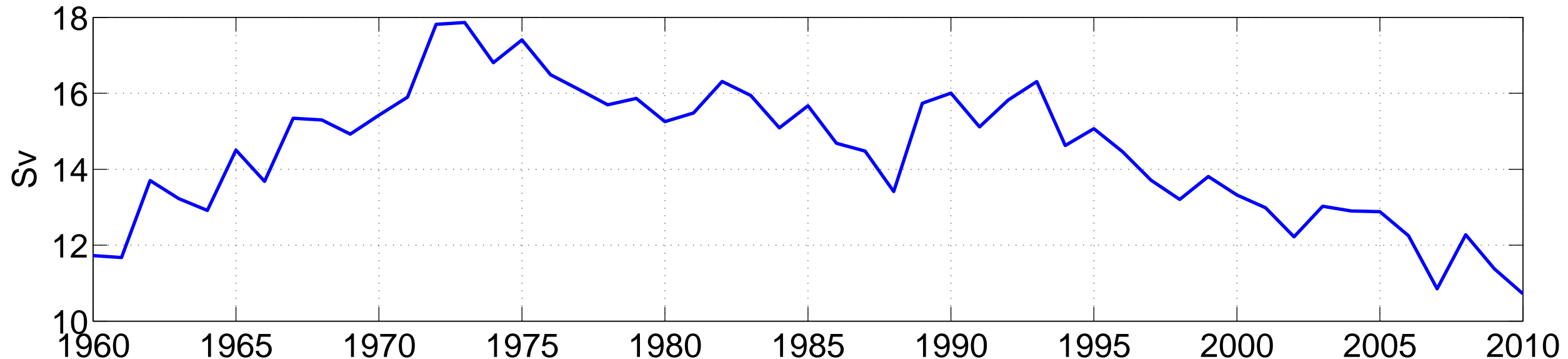
Table 1. Hosing experiments

experiment	areas of ice mass loss	rate (Gt/yr)
1	Greenland	200
2	Alaska Glaciers	50
3	West Antarctica	100
4	Greenland, Alaska Glaciers, West Antarctica	200, 50, 100
5	Greenland, West Antarctica	200, 100

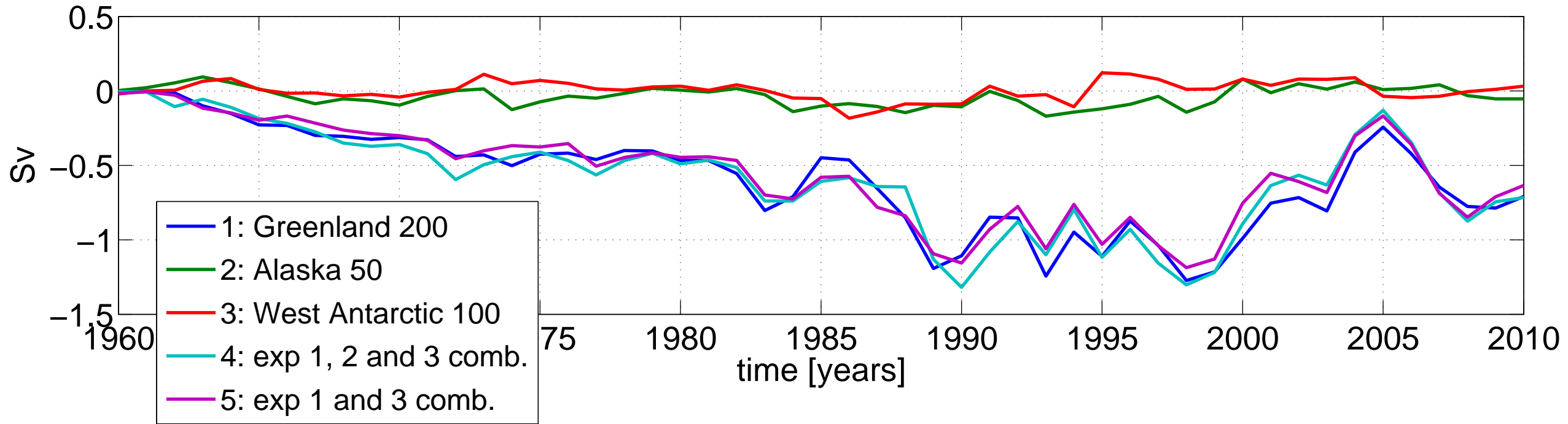


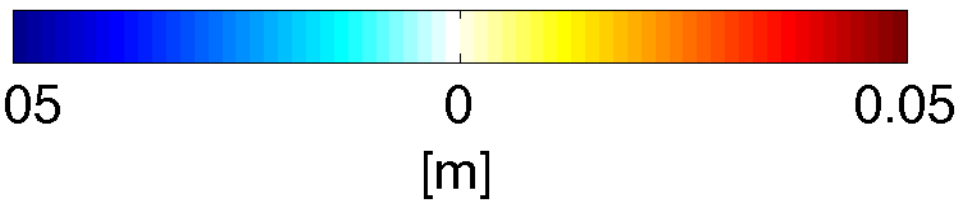
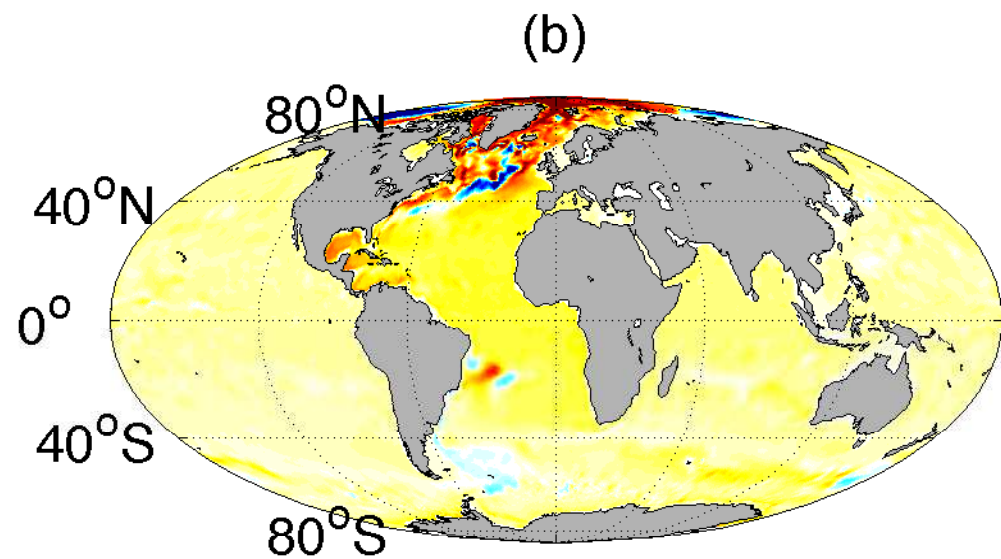
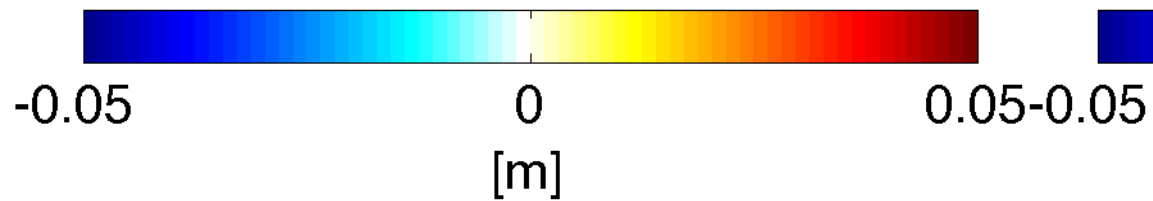
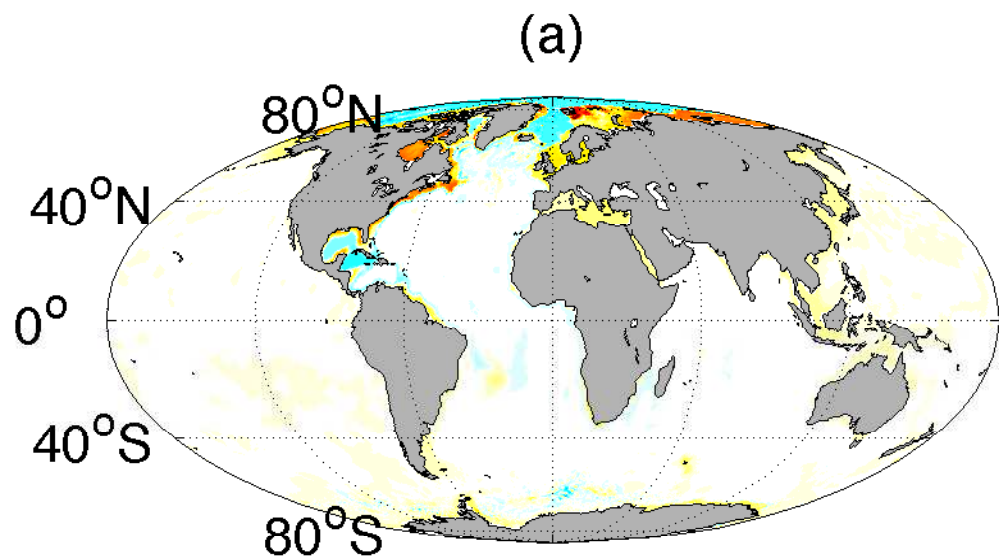


(a)

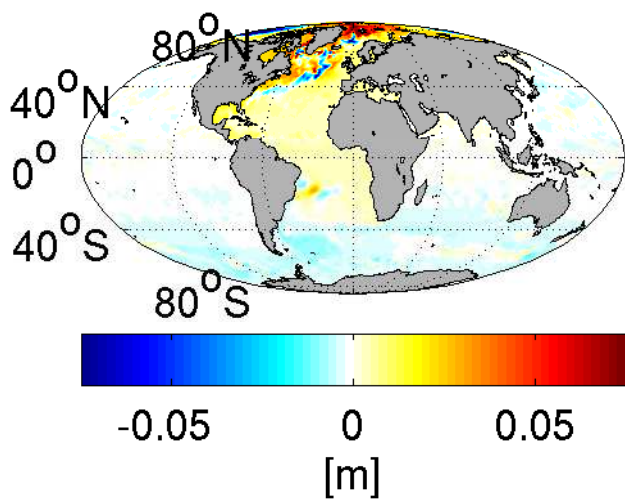


(b)

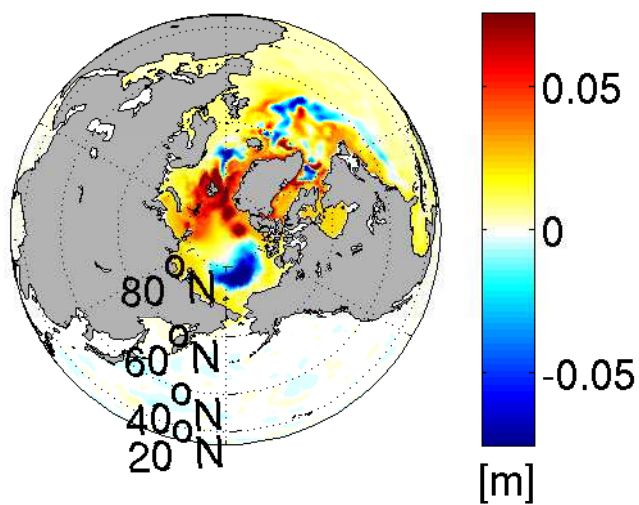




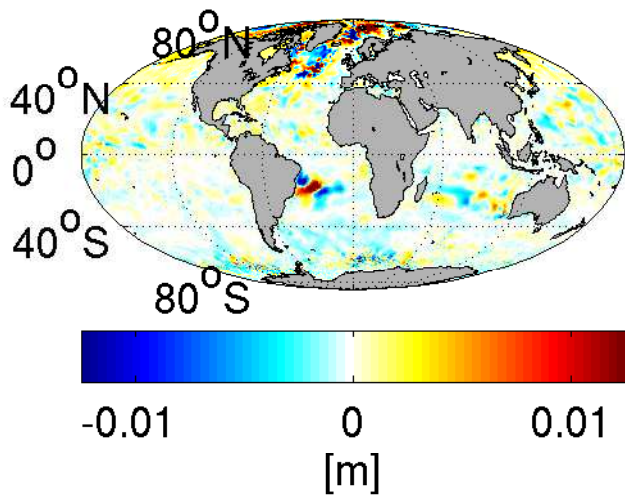
(a)



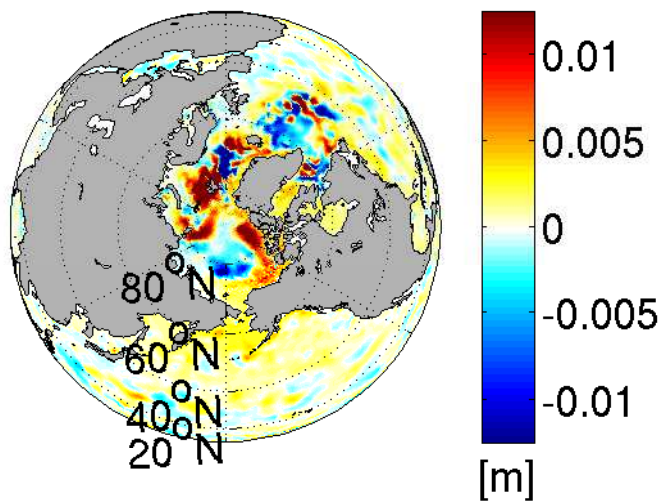
(b)



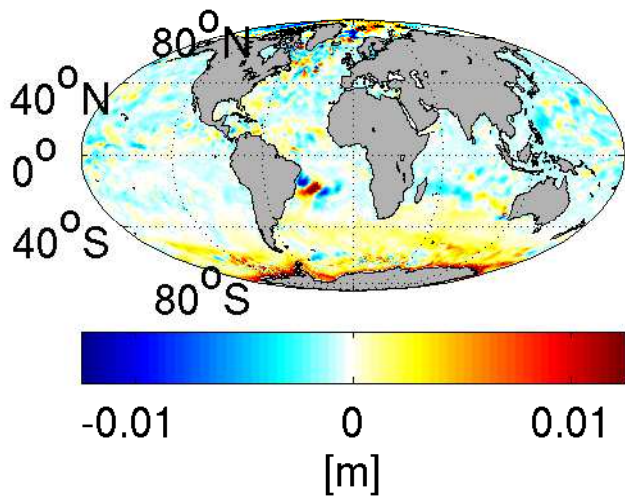
(c)



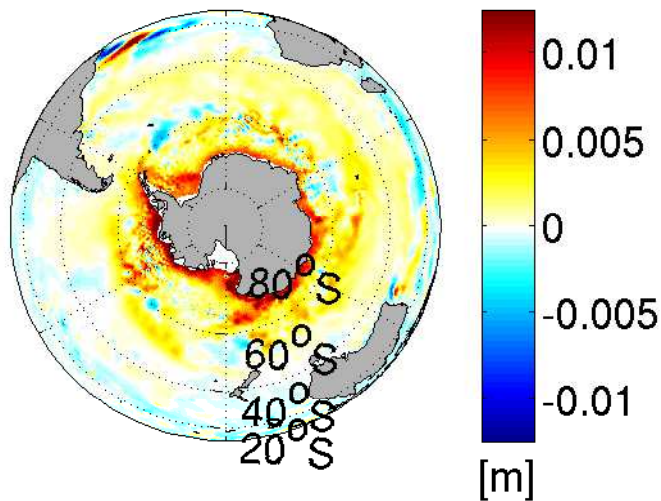
(d)



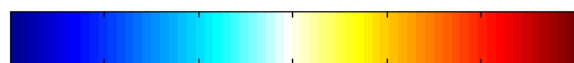
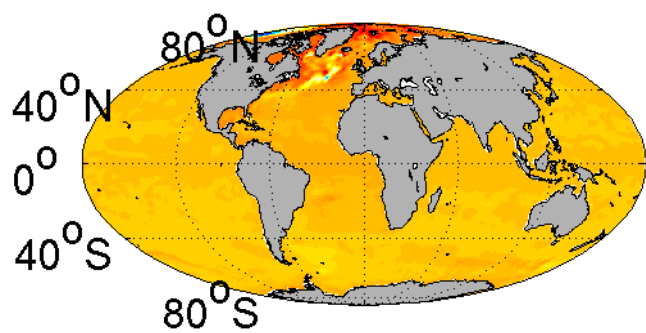
(e)



(f)

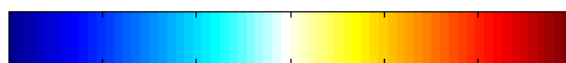
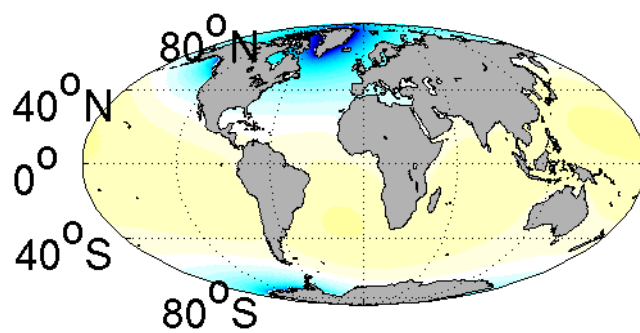


(a)



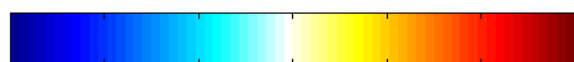
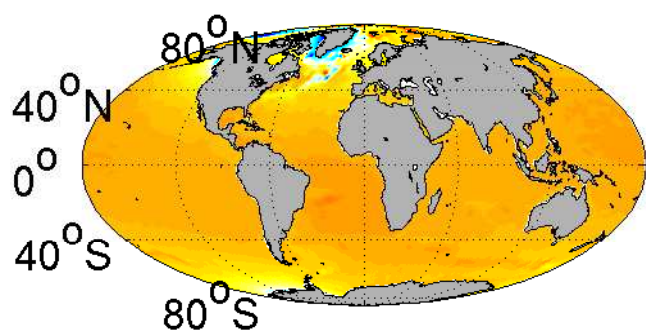
-0.1 -0.05 0 0.05 0.1
[m]

(b)



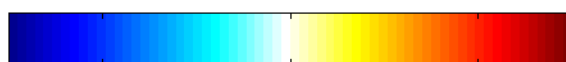
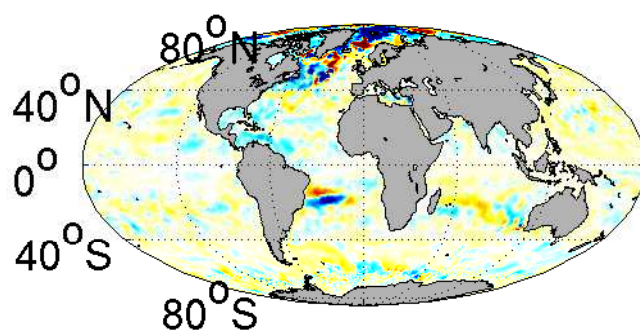
-0.1 -0.05 0 0.05 0.1
[m]

(c)



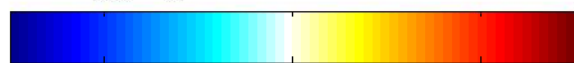
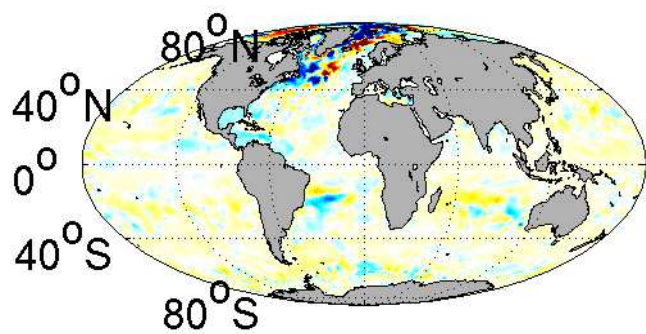
-0.1 -0.05 0 0.05 0.1
[m]

(d)



-0.01 0 0.01
[m]

(e)



-0.01 0 0.01
[m]

